

## One-Pot and Sequential Organic Chemistry on an Enzyme Surface to Tether a Fluorescent Probe at the Proximity of the Active Site with Restoring Enzyme Activity

Yousuke Takaoka,<sup>§</sup> Hiroshi Tsutsumi,<sup>‡</sup> Noriyuki Kasagi,<sup>§</sup> Eiji Nakata,<sup>†</sup> and Itaru Hamachi<sup>\*†‡</sup>

Contribution from the Department of Synthetic Chemistry and Biological Chemistry, Graduate School of Engineering, Kyoto University, Kyotodaigaku-katsura, Nishikyo-ku, Kyoto 615-8510, Japan, PRESTO (Synthesis and Control, JST), and Department of Chemistry and Biochemistry, Graduate School of Engineering, Kyushu University, Fukuoka 812-8581, Japan

Received November 22, 2005; E-mail: ihamachi@sbchem.kyoto-u.ac.jp

**Abstract:** A new and simple method to tether a functional molecule at the proximity of the active site of an enzyme has been successfully developed without any activity loss. The one-pot sequential reaction was conducted on a surface of human carbonic anhydrase II (hCAII) based on the affinity labeling and the subsequent hydrazone/oxime exchange reaction. The reaction proceeds in a greater than 90% yield in the overall steps under mild conditions. The enzymatic activity assay demonstrated that the release of the affinity ligand from the active site of hCAII concurrently occurred with the replacement by the aminoxy derivatives, so that it restored the enzymatic activity from the completely suppressed state of the labeled hCAII. Such restoring of the activity upon the sequential modification is quite unique compared to conventional affinity labeling methods. The peptide mapping experiment revealed that the labeling reaction was selectively directed to His-3 or His-4, located on a protein surface proximal to the active site. When the fluorescent probe was tethered using the present sequential chemistry, the engineered hCAII can act as a fluorescent biosensor toward the hCAII inhibitors. This clearly indicates the two advantages of this method, that is (i) the modification is directed to the proximity of the active site and (ii) the sequential reaction re-opens the active site cavity of the target enzyme.

### Introduction

There is considerable desire for useful chemical methods that can modify proteins under physiological conditions with high site- and chemoselectivities in the field of protein engineering and chemical biology.<sup>1</sup> In the case of synthetic or semisynthetic proteins, several selective reactions have been developed recently using artificially incorporated bio-orthogonal reactive tags. For example, the reaction of an unnatural amino acid bearing a ketone with hydrazides or aminoxy compounds was reported.<sup>2</sup> Schultz et al. demonstrated that ketone amino acids incorporated by a genetically modulated codon method<sup>3</sup> could be employed as a tag for chemical modification.<sup>4</sup> More recently,

they and other groups incorporated unnatural amino acids containing azide or acetylene into proteins and used them as a selective modification site for the Huisgen [3+2] cycloaddition developed by Sharpless et al.<sup>5</sup> and Finn et al.<sup>6</sup> on a protein surface.<sup>7</sup> In addition, another azide-based chemistry such as Staudinger ligation has been explored to modify proteins by Bertozzi<sup>8</sup> and Raines.<sup>9</sup> It is undoubted that these bio-orthogonal reactions have expanded chemical strategies for the selective

<sup>†</sup> Kyoto University.

<sup>‡</sup> PRESTO (Synthesis and Control, JST).

<sup>§</sup> Kyushu University.

(1) (a) Zhang, J.; Campbell, R. E.; Ting, A. Y.; Tsien, R. Y. *Nat. Rev. Mol. Cell Biol.* **2002**, *3*, 906–918. (b) Chen, L.; Ting, A. Y. *Curr. Opin. Biotechnol.* **2005**, *16*, 35–40. (c) Miller, L. W.; Cornish, V. W. *Curr. Opin. Chem. Biol.* **2005**, *9*, 56–61. (d) Johnsson, N.; Johnsson, K. *ChemBioChem* **2003**, *4*, 803–810. (e) Johnsson, N.; George, N.; Johnsson, K. *ChemBioChem* **2005**, *6*, 47–52.

(2) (a) Cornish, V. W.; Hahn, K. M.; Schultz, P. G. *J. Am. Chem. Soc.* **1996**, *118*, 8150–8151. (b) Mahal, L. K.; Yarema, K. J.; Bertozzi, C. R. *Science* **1997**, *276*, 1125–1128. (c) Datta, D.; Wang, P.; Carrico, I. S.; Mayo, S. L.; Tirrell, D. A. *J. Am. Chem. Soc.* **2002**, *124*, 5652–5653. (d) Liu, H.; Wang, L.; Brock, A.; Wong, C.; Schultz, P. G. *J. Am. Chem. Soc.* **2003**, *125*, 1702–1703. (e) Chen, I.; Howarth, M.; Lin, W.; Ting, A. Y. *Nat. Methods* **2005**, *2*, 99–104.

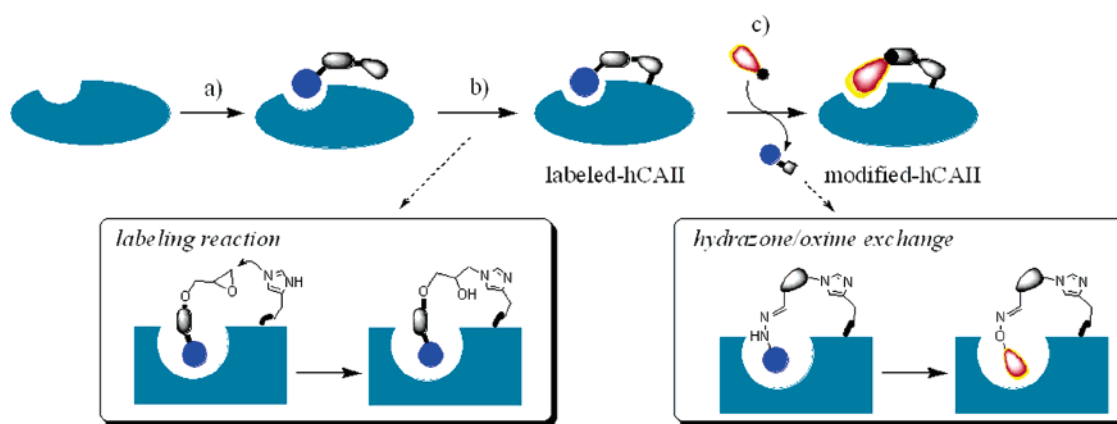
(3) (a) Wang, L.; Brock, A.; Herberich, B.; Schultz, P. G. *Science* **2001**, *292*, 498–500. (b) Chin, J. W.; Santoro, S. W.; Martin, A. B.; King, D. S.; Wang, L.; Schultz, P. G. *J. Am. Chem. Soc.* **2002**, *124*, 9026–9027. (c) Chin, J. W.; Martin, A. B.; King, D. S.; Wang, L.; Schultz, P. G. *Proc. Natl. Acad. Sci. U.S.A.* **2002**, *99*, 11020–11024. (d) Hoshida, T.; Kajihara, D.; Ashizuka, Y.; Murakami, H.; Sisido, M. *J. Am. Chem. Soc.* **1999**, *121*, 34–40.

(4) (a) Wang, L.; Zhang, Z.; Brock, A.; Schultz, P. G. *Proc. Natl. Acad. Sci. U.S.A.* **2003**, *100*, 56–61. (b) Zhang, Z.; Smith, B. A.; Wang, L.; Brock, A.; Cho, C.; Schultz, P. G. *Biochemistry* **2003**, *42*, 6735–6746.

(5) (a) Lewis, W. G.; Green, L. G.; Grynszpan, F.; Radic, Z.; Carlier, P. R.; Taylor, P.; Finn, M. G.; Sharpless, K. B. *Angew. Chem., Int. Ed.* **2002**, *41*, 1053–1057. (b) Rostovtsev, V. V.; Green, L. G.; Fokin, V. V.; Sharpless, K. B. *Angew. Chem., Int. Ed.* **2002**, *41*, 2596–2599.

(6) (a) Gupta, S. S.; Kuzelka, J.; Singh, P.; Lewis, G.; Manchester, M.; Finn, M. G. *Bioconjugate Chem.* **2005**, *16*, 1572–1579. (b) Wang, Q.; Chan, T. R.; Hilgraf, R.; Fokin, V. V.; Sharpless, K. B.; Finn, M. G. *J. Am. Chem. Soc.* **2003**, *125*, 3192–3193.

(7) (a) Deiters, A.; Cropp, T. A.; Mukherji, M.; Chin, J. W.; Anderson, J. C.; Schultz, P. G. *J. Am. Chem. Soc.* **2003**, *125*, 11782–11783. (b) Speers, A. E.; Adam, G. C.; Cravatt, B. F. *J. Am. Chem. Soc.* **2003**, *125*, 4686–4687. (c) Link, A. J.; Vink, M. K. S.; Tirrell, D. A. *J. Am. Chem. Soc.* **2004**, *126*, 10598–10602. (d) Beatty, K. E.; Xie, F.; Wang, Q.; Tirrell, D. A. *J. Am. Chem. Soc.* **2005**, *127*, 14150–14151.

**Scheme 1.** P-ALM Scheme for the Selective Modification of a Protein<sup>a</sup>

<sup>a</sup> (a) Complex formation between hCAII and P-ALM reagent. (b) The affinity labeling reaction via the epoxide ring opening to generate the labeled hCAII. (c) The step to produce the modified hCAII by the hydrazone/oxime exchange reaction.

labeling of various proteins although a genetic mutation is required during the initial stage for these modifications in many cases.

For a native protein as a target, on the other hand, limited kinds of reactions have been developed which involve a covalent bond formation between nucleophilic groups such as a cysteine or a lysine on protein surfaces and external artificial reactive groups. Although interesting tyrosine-directed azo-coupling and Mannich reactions have very recently been reported by Francis et al.,<sup>10</sup> these are still rare examples. This is because it is difficult to recognize a protein surface for site-selective reactions, in addition to the poor development of bio-orthogonal reactions conducted under physiological conditions.

We recently reported a new method (P-PALM method) based on photoaffinity labeling to incorporate a unique chemoselective tag proximal to the active site of a lectin, i.e., a saccharide-binding protein.<sup>11</sup> This is beneficial from the viewpoint that the active site-directed introduction of a chemical tag to naturally occurring proteins is potentially carried out without the use of genetically engineered proteins. However, thiol chemistry on the protein surface previously reported by us is not sufficiently general because this method is not applicable to many proteins which have cysteine residues. Another drawback of P-PALM is that the tedious and time-consuming purification procedures including several steps are needed to remove the reagents and other byproducts. A simpler modification method is most preferable.

During exploration of a general and efficient methodology, we have developed a one-pot sequential chemistry (the so-called Post-Affinity Labeling Modification: P-ALM) based on the affinity labeling modification followed by the hydrazone/oxime exchange reaction. Human carbonic anhydrase II (hCAII) was labeled at two selective positions proximal to the active site using epoxide-based P-ALM reagents having a suitable spacer length, and subsequently, the masking ligand was cleaved off using the hydrazone/oxime exchange under one-pot conditions in over 90% yield. This exchange process restores the enzyme activity of hCAII. More interestingly, we demonstrated that several fluorophores were successfully attached to hCAII by the present exchange reaction using fluorescent aminoxy derivatives, and the resultant modified hCAIIs act as fluorescent biosensors that can sense sulfonamide derivatives, a family of hCAII inhibitors.

## Results and Discussion

**Modification of Human Carbonic Anhydrase II Using Sequential Reaction.** In the present P-ALM, an affinity labeling reaction using epoxide<sup>12</sup> and the subsequent hydrazone/oxime exchange<sup>13</sup> are combined as a designer sequential reaction on a protein surface. Scheme 1 illustrates the strategy for the sequential reaction on the surface of a target protein, that is, the affinity labeling is directed to the modification site close to the active site and the hydrazone linkage between the ligand and the reaction site is subsequently replaced by an oxime bond. These two reactions proceed in a sequential manner under mild conditions, so that a one-pot modification can be carried out.

In a proof-of-principle experiment, human carbonic anhydrase II (hCAII) was used as a model protein.<sup>14</sup> In the design of the P-ALM reagents, benzenesulfonamide, which is a typical inhibitor of hCAII, and an epoxide moiety which was demonstrated to be a suitable electrophile for hCAII by Sames,<sup>12</sup> were used for targeting the active site of hCAII and for reacting with hCAII, respectively (Figure 1a, 1–4). These two moieties are linked by a hydrazone unit with various spacer lengths. The

- (8) (a) Kiick, K. L.; Saxon, E.; Tirrell, D. A.; Bertozzi, C. R. *Proc. Natl. Acad. Sci. U.S.A.* **2002**, *99*, 19–24. (b) Lemieux, G. A.; Graffenried, C. L.; Bertozzi, C. R. *J. Am. Chem. Soc.* **2003**, *125*, 4708–4709. (c) Saxon, E.; Bertozzi, C. R. *Science* **2000**, *287*, 2007–2010.
- (9) (a) Soellner, M. B.; Dickson, K. A.; Nilsson, B. L.; Raines, R. T. *J. Am. Chem. Soc.* **2003**, *125*, 11790–11791. (b) Nilsson, B. L.; Hondal, R. J.; Soellner, M. B.; Raines, R. T. *J. Am. Chem. Soc.* **2003**, *125*, 5268–5269.
- (10) (a) Hooker, J. M.; Kovacs, E. W.; Francis, M. B. *J. Am. Chem. Soc.* **2004**, *126*, 3718–3719. (b) Sclick, T. L.; Ernest, Z. D.; Kovacs, E. W.; Francis, M. B. *J. Am. Chem. Soc.* **2005**, *127*, 3718–3723. (c) Joshi, N. S.; Whitaker, L. R.; Francis, M. B. *J. Am. Chem. Soc.* **2004**, *126*, 15942–15943.
- (11) (a) Hamachi, I.; Nagase, T.; Shinkai, S. *J. Am. Chem. Soc.* **2000**, *122*, 12065–12066. (b) Nagase, T.; Shinkai, S.; Hamachi, I. *Chem. Commun.* **2001**, *3*, 229–230. (c) Nagase, T.; Nakata, E.; Shinkai, S.; Hamachi, I. *Chem. Eur. J.* **2003**, *9*, 3660–3669. (d) Nakata, E.; Nagase, T.; Shinkai, S.; Hamachi, I. *J. Am. Chem. Soc.* **2004**, *126*, 490–495. (e) Koshi, Y.; Nakata, E.; Hamachi, I. *ChemBioChem* **2005**, *6*, 1349–1352. (f) Nakata, E.; Koshi, Y.; Koga, E.; Katayama, Y.; Hamachi, I. *J. Am. Chem. Soc.* **2005**, *127*, 13253–13261. (g) Ojida, A.; Tsutsumi, H.; Kasagi, N.; Hamachi, I. *Tetrahedron Lett.* **2005**, *46*, 3301–3305.
- (12) Chen, G.; Heim, A.; Riether, D.; Yee, D.; Milgrom, Y.; Gawinowicz, M. A.; Sames, D. *J. Am. Chem. Soc.* **2003**, *125*, 8130–8133.
- (13) (a) Polyakov, V. A.; Nelen, M. I.; Nazarpak-Kandlousy, N.; Ryabov, A. D.; Eliseev, A. V. *J. Phys. Org. Chem.* **1999**, *12*, 357–363. (b) Goral, V.; Nelen, M. I.; Eliseev, A. V.; Lehn, J.-M. *Proc. Natl. Acad. Sci. U.S.A.* **2001**, *98*, 1347–1352. (c) Shao, H.; Crnogorac, M. M.; Kong, T.; Chen, S.-Y.; Williams, J. M.; Tack, J. M.; Gueriguian, V.; Cagle, E. N.; Carnevali, M.; Tumelty, D.; Paliard, X.; Miranda, L. P.; Bradburne, J. A.; Kochenderfer, G. G. *J. Am. Chem. Soc.* **2005**, *127*, 1350–1351.
- (14) (a) Roy, B. C.; Banerjee, A. L.; Swanson, M.; Jia, X. G.; Haldar, M. K.; Mallik, S.; Srivastava, D. K. *J. Am. Chem. Soc.* **2004**, *126*, 13206–13207. (b) Banerjee, A. L.; Swanson, M.; Roy, B. C.; Jia, X.; Haldar, M. K.; Mallik, S.; Srivastava, D. K. *J. Am. Chem. Soc.* **2004**, *126*, 10875–10883.

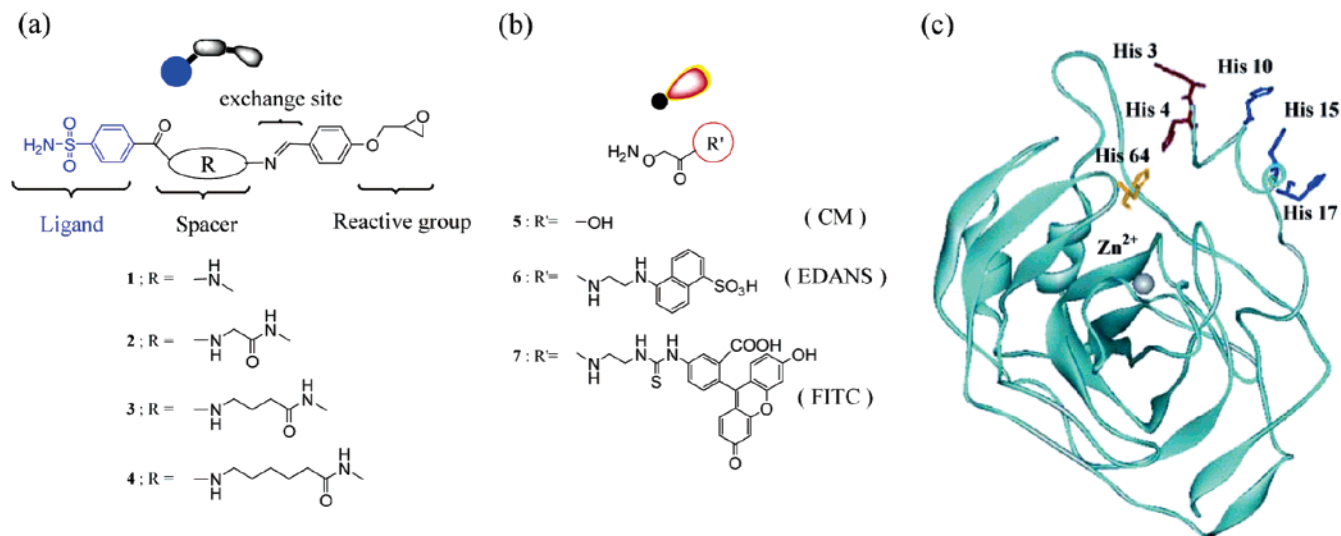


**Figure 1.** Chemical structures of (a) P-ALM reagents and (b) aminoxy derivatives used in this study. (c) Structural model of hCAII.

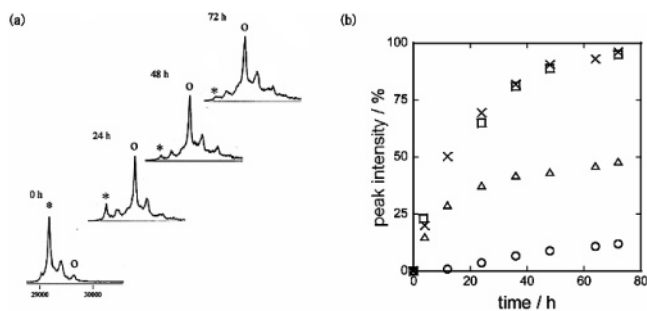


**Figure 2.** (a) MALDI-TOF mass spectra of reaction mixture of hCAII with **3** (\*; native hCAII ( $M_w$  29 057), ○; **3**-labeled-hCAII ( $M_w$  29 514), spectra changed at 0, 24, 48, and 72 h from bottom to top). (b) Time course of the labeling reaction process of hCAII with **1** (○), **2** (△), **3** (□), and **4** (×), respectively. The detail reaction conditions were described in the Experimental Section.

hydrazone can be reversibly replaced with other functionalities such as an aminoxy or hydrazine group. After **3** was mixed with hCAII in an aqueous buffer (pH 7.2), the mixture was incubated at 25 °C for 48–72 h. The reaction progress was monitored by MALDI-TOF mass spectroscopy (Figure 2a and 2b), showing the almost total completion of the labeling reaction (**3**-labeled-hCAII) within 48 h (□). In the case of the P-ALM reagent **4** (◆) having the longer spacer, the labeling reaction was completed within 48 h similar to **3**. In contrast, the reaction using **2** (△) less efficiently proceeded to only 50%, and **1** (○) gave less than 10% of the **1**-labeled-hCAII after the 72 h incubation. It is clear that the yield in the labeling step significantly depends on the methylene length between the sulfonamide site and the reactive epoxide site of the P-ALM reagent (Figure 1a,c). The two or more modifications of hCAII were not observed in the MALDI-TOF data, indicating that the single-site modification predominantly took place in this method. As control experiments, neither reaction using an epoxide lacking the sulfonamide part, nor the reaction with **3** in the presence of 10 equiv of a strong inhibitor, 6-ethoxy-2-benzothiazolesulfonamide (ET),<sup>15</sup> afforded the labeled hCAII. These results strongly suggest that the present labeling process is effectively assisted by the ligand binding of **3** to the active site pocket of hCAII.

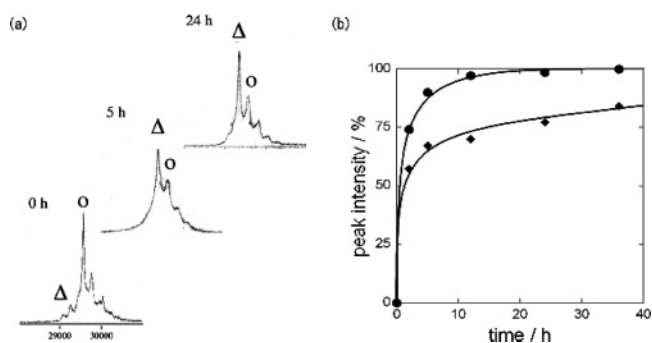


**Figure 3.** (a) MALDI-TOF mass spectra of reaction mixture of **3**-labeled-hCAII with 100 equiv of **5** at 45 °C, pH 5.5 (○; **3**-labeled-hCAII ( $M_w$  29 514), △; CM-hCAII ( $M_w$  29 308), spectra changed at 0, 5, and 24 h from bottom to top). (b) Time course of the hydrazone/oxime exchange reaction process of **3**-labeled-hCAII in the presence of 100 equiv of **5** at 45 °C, pH 5.5 (●), pH 7.2 (◆).

After the labeling reaction (**3**-labeled hCAII), carboxymethyl-oxyamine (CM) **5** was added to the labeled reaction mixture at various concentrations, and then the reaction mixture was incubated at various pHs and temperatures to determine the optimal conditions. All modified hCAIIs were purified by gel-filtration chromatography before analyzing the function (details are described in the Experimental Section). The hydrazone/oxime exchange reaction was again traced by MALDI-TOF MS, showing that the exchange reaction at pH 5.5 was almost completed within less than 24 h in the presence of 100 equiv of **5** (Figure 3). For the reaction at neutral pH (pH 7.2), on the other hand, the yield slightly decreased to 77% at 45 °C for 24 h or 73% (at 25 °C), and it significantly decreased to 43–30% under more basic conditions (pH 9.0). Table 1 summarizes the yields of the reaction under various conditions, indicating that (i) the reaction efficiently proceeds under acidic pH conditions, due to acceleration of the proton-assisted exchange reaction, (ii) the excess amount of the aminoxy group is needed for the good conversion, and (iii) the reaction yield is not very sensitive to the reaction temperature. At the more acidic pH (pH = 4) and/or the higher temperature (at 50 °C), the isolation yield

(15) Casini, A.; Antel, J.; Abbate, F.; Scozzafava, A.; David, S.; Waldeck, H.; Schäfer, S.; Supuran, C. T. *Bioorg. Med. Chem. Lett.* **2003**, *13*, 841–845.

**Table 1.** Yields of the One-Pot Sequential Reaction under Various Conditions for 24 h

aminoxy derivatives	temp (°C)	quantity (equiv)	yield (%)		
			pH 5.5	pH 7.2	pH 9.0
CM	25	100	83 <sup>a</sup>	73 <sup>a</sup>	<i>c</i>
	45	20	84 <sup>a</sup>	43 <sup>a</sup>	30 <sup>a</sup>
	45	100	>95 <sup>a</sup>	77 <sup>a</sup>	43 <sup>a</sup>
EDANS	45	20	77 <sup>b</sup>	<i>c</i>	<i>c</i>
FITC	45	20	78 <sup>b</sup>	<i>c</i>	<i>c</i>

<sup>a</sup> Yield determined by MALDI-TOF MS analysis. <sup>b</sup> Isolation yield determined by UV–visible spectroscopy. <sup>c</sup> Not determined.

decreased, probably due to the partial denaturation of hCAII under the rather severe reaction conditions. When the fluorescent aminoxy derivatives, such as EDANS (**6**) or FITC (**7**), were employed in the second step, a fluorescent probe was successfully introduced to hCAII in a similar manner (the isolation yield is 77% for EDANS- and 78% for FITC-hCAII at 45 °C, pH 5.5, for 72 h). These results have demonstrated that various artificial molecules can be incorporated into natural hCAII via the aminoxy tag using the hydrazone/oxime exchange modification with good yield under mild conditions.

#### Structural Characterization of Labeled/Modified hCAII.

The labeled hCAII in the first step of the present P-ALM was characterized by MALDI-TOF mass spectroscopy, and the modified hCAII in the second step was characterized by MALDI-TOF MS, UV–visible, and fluorescence spectroscopies. The mass peaks (*m/z*) were observed at 29 432, 29 489, 29 517, and 29 545 for the **1**-, **2**-, **3**-, and **4**-labeled-hCAII, respectively. The mass peaks of the modified hCAIIs appeared at 29 308 for CM-hCAII, at 29 556 for EDANS-hCAII, and at 29 739 for FITC-hCAII, respectively. These values agree well with the sum of the *M<sub>w</sub>*'s of the native hCAII and the corresponding tagged molecules. In the UV–visible spectra of EDANS-hCAII, the absorbance at 336 nm is characteristic of the EDANS unit that appeared together with 280 nm due to hCAII. In addition, the emission maximum at 470 nm and the excitation maximum at 336 nm due to the EDANS fluorophore were clearly observed in EDANS-hCAII. Similarly, in the case of FITC-hCAII, the 494 nm absorption in the UV–vis spectrum and the 520 nm fluorescence, both due to FITC, appeared for FITC-hCAII.

The labeling site of EDANS-hCAII prepared from the **3**-labeled hCAII was determined by the conventional peptide mapping experiment using Lysyl endopeptidase (LEP) which selectively hydrolyzes peptide bonds at the C terminal site of the lysine residues.<sup>16</sup> Figure 4 shows the reversed-phase HPLC trace of the digested peptides for EDANS-hCAII monitored by the UV (Figure 4b) and fluorescence detector, compared to that of the native hCAII (Figure 4a). In the HPLC chart of the fluorescence mode (Figure 4c), two major peaks (retention time (*R<sub>t</sub>*) = 42, 44 min) and one minor peak (*R<sub>t</sub>* = 30 min) mainly appeared. The MALDI-TOF MS analysis indicates that the two major peaks had identical mass, both of which can be assigned to the EDANS modified N-terminal peptide (the N-terminal L1 fragment plus one molecule of the EDANS unit, i.e., [*M* + *H*]<sup>+</sup> = 1512). The subsequent tandem mass–mass analysis clarified that the labeling site was His-3 (*R<sub>t</sub>* = 44 min, Figure 4d) or His-4 (*R<sub>t</sub>* = 42 min, Figure S8a). On the 3D-structure of hCAII, His-3 and His-4 are exposed on the protein surface closely

connected to the active site (Figure 1c).<sup>17</sup> Therefore, it is reasonable that one of the two sites was selectively labeled by the nucleophilic ring opening of the epoxide when the labeling reagent **3** was bound to the active site of hCAII. In addition, this result was in good agreement with the detailed molecular modeling study reported by Srivastava et al.<sup>14b,18</sup> On the other hand, Sames et al. reported that His-64 of hCAII was selectively labeled using an epoxide-based affinity labeling reagent having a fluorescein unit. Since the hydrophobic fluorescein part is favorably bound to the hydrophobic crevasse close to the active site, the epoxide part might be juxtaposed toward the rather buried His-64, so that His-64 was selectively labeled in their case.<sup>12</sup> Another minor peak (*R<sub>t</sub>* = 30 min, Figure S8b) was assigned to the dehydrogenated L1-fragment conjugated with EDANS because the mass peak was observed at *m/z* = 1510, two molecular weights less than the calculated mass of the EDANS-modified L1 peptide. This may suggest that some oxidation occurred as a side reaction during or after the P-ALM reaction processes.

**Restoring Enzyme Activity by Hydrazone/Oxime Exchange Reaction.** The enzyme activities of the labeled and modified hCAIIs were examined by the conventional ester hydrolysis reaction using *p*-nitrophenyl acetate as the substrate.<sup>19</sup> The initial rates of the ester hydrolysis were measured at various substrate concentrations, and the kinetic parameters of the labeled or modified hCAIIs were determined (Figure 5 and Table 2). For the **3**-labeled-hCAII (◆), the enzymatic activity was almost perfectly suppressed so that the catalytic parameters could not be determined. This is because the benzenesulfonamide part of the P-ALM reagent efficiently masked the active site. In contrast, CM-hCAII (●) showed an activity having a *k<sub>cat</sub>* value (7.0 s<sup>-1</sup>) almost identical with that of the native hCAII (○, 6.2 s<sup>-1</sup>), clearly indicating that the closed active site was re-opened by the hydrazone/oxime exchange reaction. In the case of EDANS-hCAII (□) and FITC-hCAII (◆), the suppressed activity was partially recovered. There is not a significant decrease in the *k<sub>cat</sub>* values of EDANS- (3.8 s<sup>-1</sup>) and FITC-hCAII (4.5 s<sup>-1</sup>) relative to the native hCAII (6.2 s<sup>-1</sup>), whereas the substrate binding affinity (1/*K<sub>m</sub>*) of EDANS- (4.85 × 10<sup>2</sup> M<sup>-1</sup>) and FITC-hCAII (4.55 × 10<sup>2</sup> M<sup>-1</sup>) was reduced to 22 and 20% relative to that of the native hCAII (2.25 × 10<sup>3</sup> M<sup>-1</sup>), respectively. The CM-hCAII tethering the simple aminoxy acetic acid, which is much smaller than the EDANS- and FITC-group, showed an intermediate 1/*K<sub>m</sub>* value (9.15 × 10<sup>2</sup> M<sup>-1</sup>) between the native hCAII and EDANS-/FITC-hCAII. In addition, the specificity constants (*k<sub>cat</sub>*/*K<sub>m</sub>*) of CM- (6.45 × 10<sup>3</sup> s<sup>-1</sup> M<sup>-1</sup>), EDANS- (1.85 × 10<sup>3</sup> s<sup>-1</sup> M<sup>-1</sup>), and FITC-hCAII (2.05 × 10<sup>3</sup> s<sup>-1</sup> M<sup>-1</sup>) were 46, 13, and 14% relative to that of the native hCAII (1.45 × 10<sup>4</sup> s<sup>-1</sup> M<sup>-1</sup>), respectively. These specificity constants were mainly affected by the binding affinity, not by the catalytic efficiency. As demonstrated by the fluorescent anisotropy experiment described in the next section, these

(16) Shikata, Y.; Kuwada, M.; Hayashi, Y.; Hashimoto, A.; Koide, A.; Asakawa, N. *Anal. Chim. Acta*, **1998**, *365*, 241–247.

(17) The X-ray crystallographic structure of recombinant hCAII in the presence of 4-fluorobenzenesulfonamide has been known to atomic resolution. Kim, C.-Y.; Christianson, D. W. PDB ID: 1IF4.

(18) Upon performing the energy minimization of P-ALM reagent **1**, **2**, **3**, and **4**, it was noted that the distance between the NH<sub>2</sub> nitrogen of benzenesulfonamide and the epoxide ring was 14, 16, 20, and 23 Å for **1**, **2**, **3**, and **4**, respectively. By the way, the linear distance between the zinc atom of the active site and the Ne2 nitrogen of the surface-exposed histidine for His-64, His-4, and His-3 was determined to be 12, 15, and 24 Å, respectively.<sup>14b</sup>

(19) (a) Elleby, B.; Sjöblom, B.; Lindskog, S. *Eur. J. Biochem.* **1999**, *262*, 516–521. (b) Pocker, Y.; Stone, J. T. *Biochemistry* **1967**, *6*, 668–678.

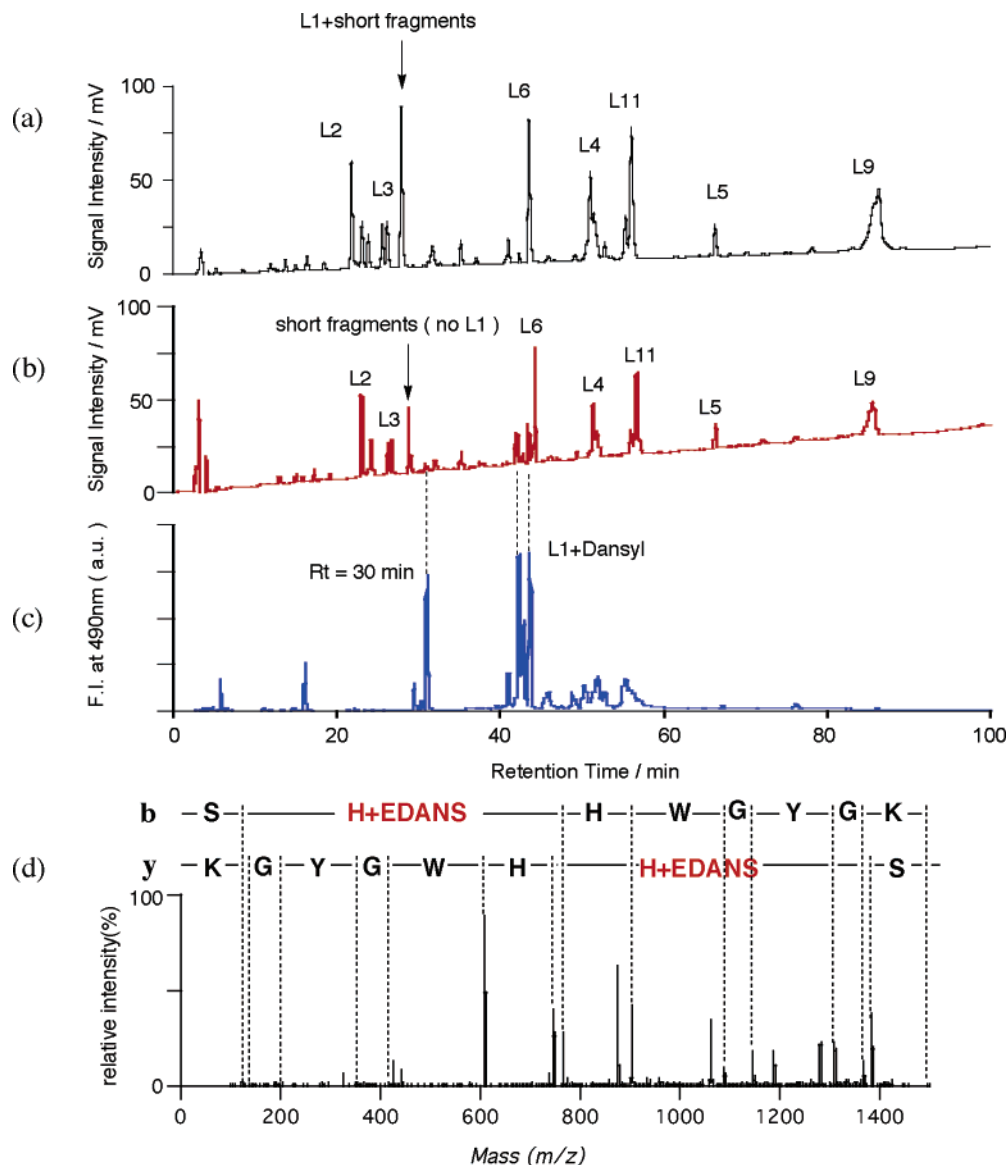


**Figure 4.** (a) HPLC analysis of native hCAII fragments monitored by UV detector. EDANS-hCAII fragments monitored by (b) UV detector and (c) fluorescence detector ( $\lambda_{\text{ex}} = 340 \text{ nm}$ ,  $\lambda_{\text{em}} = 490 \text{ nm}$ ). (d) Tandem mass–mass analysis of the EDANS-labeled fragment ( $R_t = 44 \text{ min}$ ). The full amino acid sequence of native hCAII was shown in Figure S7. L1–L11 are fragments of native and EDANS-hCAII hydrolyzed by lysyl endopeptidase.

fluorophores should locate in the hydrophobic pocket proximal to the substrate binding site.<sup>20</sup> Therefore, it is plausible that the bulky fluorophore tethering to the hCAII surface proximal to the active site may partially block the substrate entry.

#### Function of a Modified hCAII as a Fluorescent Biosensor.

As already-mentioned, the present P-ALM method can maintain the active site of hCAII while a fluorescent probe is attached to the proximity of the active site. This unique advantage was utilized for the development of a fluorescent biosensor on the basis of the hCAII scaffold. Figure 6a shows the typical fluorescence spectral change in EDANS-hCAII by the addition of 4-sulfamoylbenzoic Acid (SA). The emission maximum at 470 nm due to the EDANS fluorophore was slightly red-shifted to 477 nm with the concurrent decrease in the emission intensity. Such a spectral change clearly implies that the EDANS moiety,

which was weakly bound to the hydrophobic environment of the active site in the absence of SA, was turned out upon SA binding.<sup>11b, 21</sup> This mechanism is consistently supported by the fluorescence anisotropy measurement with or without the SA binding (Figure S10). That is, in the absence of SA, the anisotropy parameter ( $r$ ) of EDANS-hCAII was 0.158, and it decreased to be 0.063 with the addition of SA in the saturation manner. The fluorescence titration curve also showed the typical saturation behavior, producing the binding constant of  $8.85 \times 10^5 \text{ M}^{-1}$  for SA. As shown in Figure 6b, similar titration curves were obtained by the addition of the sulfonamide family ( $>10^6 \text{ M}^{-1}$  for ET,  $>10^6 \text{ M}^{-1}$  for NB,  $3.65 \times 10^5 \text{ M}^{-1}$  for BS,  $1.25 \times 10^3 \text{ M}^{-1}$  for SA1. The molecular structures are summarized in Figure 6c), whereas SA2 never induced the fluorescence change (the binding constant was too low to be determined). A similar spectral change was observed in the case of FITC-hCAII

(20) (a) Pocker, Y.; Storm, D. R. *Biochemistry* **1968**, *7*, 1202–1212. (b) Chênevert, R.; Rhlid, R. B.; Létourneau, M.; Gagnon, R.; D'Astous, L. *Tetrahedron: Asymmetry* **1993**, *4*, 1137–1140. (c) Grüneberg, S.; Stubbs, M. T.; Klebe, G. *J. Med. Chem.* **2002**, *45*, 3588–3602.

(21) Enander, K.; Dolphin, G. T.; Liedbreg, B.; Lundstrom, I.; Baltzer, L. *Chem. Eur. J.* **2004**, *10*, 2375–2385.

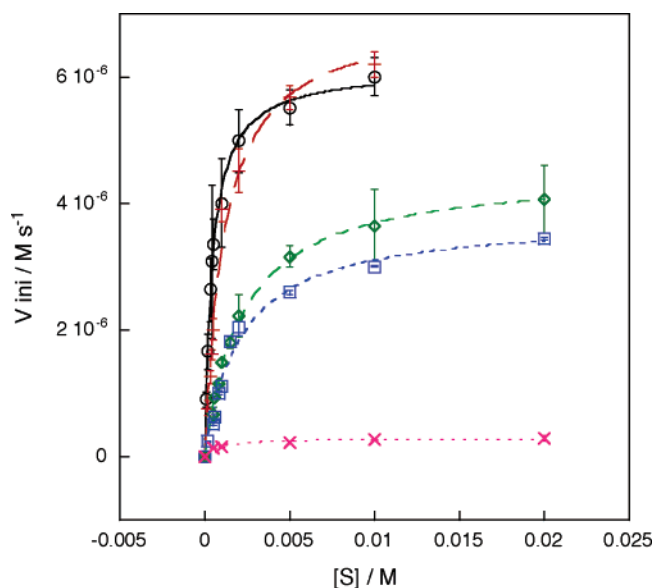


**Figure 5.** Michaelis–Menten for hydrolysis of *p*-nitrophenyl acetate catalyzed by native hCAII (○), 3-labeled-hCAII (×), CM-hCAII (●), EDANS-hCAII (□) and FITC-hCAII (◆), respectively. The concentration of hCAIIs was fixed at 1.0 μM. The concentration of *p*-nitrophenyl acetate was varied from 0.1 to 20 mM. The lines were obtained by least-squares curve-fitting analysis using the Michaelis–Menten equation.

**Table 2.** Kinetic Parameters of Native hCAII, 3-labeled-hCAII, CM-hCAII, EDANS-hCAII, and FITC-hCAII for the Hydrolysis of *p*-Nitrophenyl Acetate

hCAII derivatives	kinetic parameters		
	$k_{\text{cat}}$ (s <sup>-1</sup> )	$1/K_m$ (M <sup>-1</sup> )	$k_{\text{cat}}/K_m$ (s <sup>-1</sup> M <sup>-1</sup> )
native	6.2	$2.2 \times 10^3$	$1.4 \times 10^4$
3-labeled	n.d. <sup>a</sup>	n.d. <sup>a</sup>	n.d. <sup>a</sup>
CM-modified	7.0	$9.1 \times 10^2$	$6.4 \times 10^3$
EDANS-modified	3.8	$4.8 \times 10^2$	$1.8 \times 10^3$
FITC-modified	4.5	$4.5 \times 10^2$	$2.0 \times 10^3$

<sup>a</sup> n.d. = not determined due to the low reactivity.

(Figure S9), and Table 3 summarizes the association constants of the modified hCAII for various benzenesulfonamide derivatives, together with those of the native hCAII.<sup>15,22</sup> It is clear that the orders of both the inhibitor affinity and the affinity value were practically identical with that of native hCAII. As a control experiment, we prepared a randomly modified hCAII with the dansyl group at some lysine residues. No significant changes in the fluorescence intensity and wavelength were induced by the addition of SA, undoubtedly indicating that the active-site-directed tethering of the fluorescent probe is essential for the fluorescence sensing of the sulfonamide derivatives in EDANS- or FITC-hCAII.

## Conclusion

In summary, we successfully developed a unique chemistry-based method to tether a fluorophore at the proximity of the active site of a naturally occurring enzyme. The one-pot sequential reaction conducted on the enzyme surface has significantly simplified the tedious modification procedure without any genetic techniques. The removal of the ligand part from the active site was concurrently achieved with the hy-

drazone/oxime exchange reaction so as to restore the enzyme activity. Such an activity recovery upon the sequential modification is advantageous over the conventional affinity labeling methods, so that one can use (or visualize) the modified enzyme bearing the original function. As a proof-of-principle example, a fluorescent biosensor based on the enzyme scaffold was successfully produced by P-ALM. These features potentially expand the present chemical method to various proteins including the disulfide bond or cysteine-containing proteins, and thus we might apply this method not only in a test tube but also inside or on the surface of a living cell with appropriate improvement.

## Experimental Section

**Materials and Methods.** Human carbonic anhydrase II (isozyme) and lysyl endopeptidase were purchased from Sigma and Wako Pure Chemical Industries, Ltd., respectively. Other chemicals and solvents were purchased from Tokyo Kasei Kogyo, Co. Ltd., or Aldrich and used without further purification. Matrix-assisted laser desorption/ionization time-of-flight mass spectrometry (MALDI-TOF MS) was recorded on PE Voyager DE-RP or Bruker Daltonics autoflex, where sinapic acid and α-cyano-4-hydroxycinnamic acid were used as a matrix. HPLC was carried out on a reversed-phase column (Hitachi L-7100 HPLC system). UV-vis spectra were recorded on a Shimadzu UV-visible 2550 spectrometer. Fluorescence spectra were recorded on a Perkin-Elmer LS55 spectrometer equipped with polarizer.

**Synthesis of the P-ALM Reagent 3.** To a suspension of 4-sulfamoylbenzoic acid (1.00 g, 5.00 mmol) in 10 mL of dry dimethylformamide solution containing WSC HCl (1.15 g, 6.00 mmol), HOBt·H<sub>2</sub>O (913 mg, 6.00 mmol), and DIPEA (2.17 mL, 12.5 mmol) was added methyl 4-aminobutyrate hydrochloride (917 mg, 6.00 mmol). After the reaction mixture was stirred at room temperature for 3 h, the solution was diluted with 50 mL of water. The aqueous solution was extracted with ethyl acetate (3×30 mL), and the extract was washed with brine, dried over anhydrous MgSO<sub>4</sub>, and concentrated under reduced pressure. The oily residue was precipitated with CHCl<sub>3</sub> to give 4-(4-sulfamoylbenzoylamino)butyric acid methyl ester as a white solid (1.19 g, 80%). <sup>1</sup>H NMR (400 MHz, CD<sub>3</sub>OD): δ/ppm 7.95 (m, 4H), 3.42 (m, 2H), 2.41 (m, 2H), 1.93 (m, 2H).

To a suspension of 4-(4-sulfamoylbenzoylamino)butyric acid methyl ester (500 mg, 1.7 mmol) in 5 mL of dry dimethylformamide was added hydrazine monohydrate (83 mg, 2.0 mmol), and the reaction mixture was stirred at room temperature for 12 h. The solution was evaporated, and then the residue was precipitated by ethyl acetate to give *N*-(3-hydrazinocarbonyl-propyl)-4-sulfamoylbenzamide as a white solid (450 mg, 90%). <sup>1</sup>H NMR (400 MHz, CD<sub>3</sub>OD): δ/ppm 7.96 (m, 4H), 3.41 (m, 2H), 2.25 (m, 2H), 1.93 (m, 2H).

4-Oxiranylmethoxybenzaldehyde (40 mg, 0.22 mmol) which was prepared according to the literature,<sup>23</sup> was mixed with *N*-(3-hydrazinocarbonylpropyl)-4-sulfamoylbenzamide (67 mg, 0.22 mmol) in 0.5 mL of dry dimethylformamide. The reaction mixture was stirred at room temperature for 12 h, and the solution was evaporated. The oily residue was precipitated with cooled methanol to give the P-ALM reagent **3** as a white solid (80 mg, 78%). <sup>1</sup>H NMR (400 MHz, DMSO-*d*<sub>6</sub>): δ/ppm 8.68 (m, 1H), 8.01 (d, *J*<sub>H</sub> = 8.4 Hz, 2H), 7.89 (d, *J*<sub>H</sub> = 8.4 Hz, 2H), 7.45 (d, *J*<sub>H</sub> = 8.8 Hz, 2H), 7.00 (d, *J*<sub>H</sub> = 8.8 Hz, 2H), 4.38 (m, 1H), 3.85 (m, 1H), 3.41 (m, 2H), 3.35 (m, 1H), 2.84 (m, 1H), 2.69 (m, 1H), 2.66 (m, 1H), 2.25 (m, 2H), 1.85 (m, 2H). HRMS (FAB<sup>+</sup>) calculated for C<sub>21</sub>H<sub>25</sub>N<sub>4</sub>O<sub>6</sub>S *m/z* 461.1495, observed *m/z* 461.1508

Elementary analysis: calculated for C<sub>21</sub>H<sub>24</sub>N<sub>4</sub>O<sub>6</sub>S: C, 54.77; H, 5.25; N, 12.17. Found: C, 54.62; H, 5.25; N, 12.07.

(22) (a) Taylor, P. W.; King, R. W.; Burgen, A. S. V. *Biochemistry* **1970**, *9*, 2638–2645. (b) Innocenti, A.; Zimmerman, S.; Ferry, J. G.; Scozzafava, A.; Supuran, C. T. *Bioorg. Med. Chem. Lett.* **2004**, *14*, 4563–4567.

(23) Kitaori, K.; Furukawa, Y.; Yoshimoto, H.; Otera, J. *Tetrahedron* **1999**, *55*, 14381–14390.

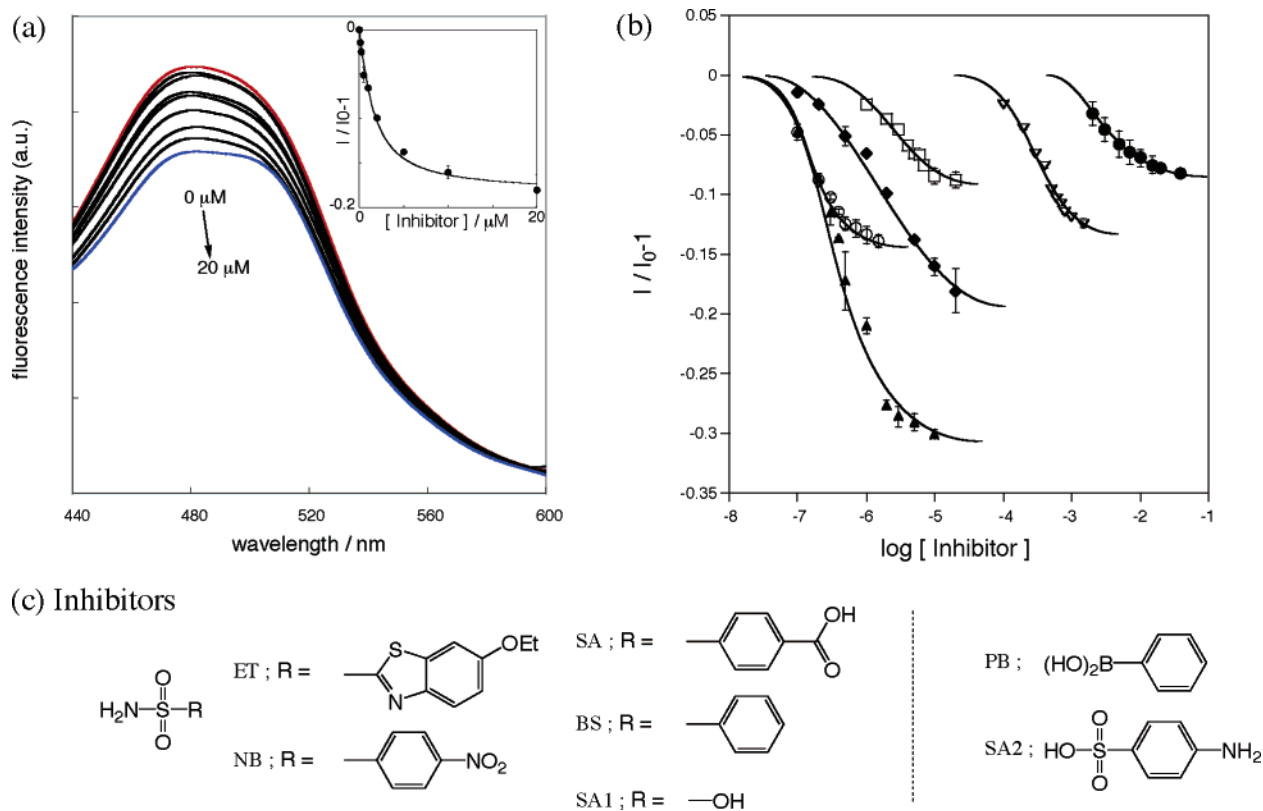


**Figure 6.** (a) Fluorescence spectral change of EDANS-hCAII upon the addition of SA: [SA] = 0, 0.5, 1.0, 1.5, 2.0, 2.5, 5, 10, 20  $\mu\text{M}$  (from top to bottom). (Inset) Titration curve of EDANS-hCAII with SA.  $I$  and  $I_0$  represent the fluorescent intensity at various inhibitor concentrations and the initial fluorescent intensity, respectively. The solid line was obtained with the nonlinear curve-fitting analysis. (b) Fluorescence titration profile of the relative intensity change ( $I/I_0 - 1$ ) versus the inhibitor concentration for EDANS-hCAII with ET(○), NB(▲), SA(◆), BS(□), SA1(▽), PB(●). (c) Chemical structure of the inhibitors for hCAII used in this study. The abbreviations are ET: 6-ethoxy-2-benzothiazolesulfonamid; NB: 4-nitrobenzenesulfonamide; SA: 4-sulfamoylbenzoic acid; BS: benzenesulfonamide; SA1: sulfamic acid; PB: phenylboronic acid; SA2: sulfanilic acid.

**Table 3.** Association Constants of EDANS-hCAII, FITC-hCAII, and Native hCAII for Various Inhibitors

inhibitors	$K_d/M^{-1}$		
	EDANS-hCAII <sup>a</sup>	FITC-hCAII <sup>a</sup>	native hCAII <sup>b</sup>
ET	$>10^6$	$>10^{7c}$	$1.3 \times 10^8$
NB	$>10^6$	$1.4 \times 10^{7d}$	$1.6 \times 10^7$
SA	$8.8 \times 10^5$	$4.5 \times 10^5$	$3.7 \times 10^6$
BS	$3.6 \times 10^5$	$2.7 \times 10^5$	$6.5 \times 10^5$
SA1	$1.2 \times 10^3$	$1.2 \times 10^3$	$4.7 \times 10^3$
PB	$2.4 \times 10^2$	$8.3 \times 10^1$	$9.4 \times 10^1$
SA2	<i>e</i>	<i>e</i>	<i>f</i>

<sup>a</sup> Determined by the nonlinear curve-fitting analysis. <sup>b</sup> Reported values determined by the enzyme kinetics.<sup>14,20</sup> <sup>c</sup> Condition at [FITC-hCAII] = 0.1  $\mu\text{M}$ . <sup>d</sup> Condition at [FITC-hCAII] = 0.5  $\mu\text{M}$ . <sup>e</sup> Not determined due to the low affinity. <sup>f</sup> There is no literature value.

P-ALM reagent **1**, **2**, and **4** were synthesized in the same manner. Detailed experimental procedures for these compounds are supplied in Supporting Information.

**1**: yield: 23 mg (30%), <sup>1</sup>H NMR (400 MHz, DMSO-*d*<sub>6</sub>):  $\delta$ /ppm 8.63 (s, 1H), 8.05 (d,  $J_H = 8.4$  Hz, 2H), 7.93 (d,  $J_H = 8.4$  Hz, 2H), 7.80 (d,  $J_H = 8.8$  Hz, 2H), 7.07 (d,  $J_H = 8.8$  Hz, 2H), 4.42–3.90 (m, 2H), 3.41 (m, 1H), 2.85, 2.72 (m, 2H). HRMS (FAB<sup>+</sup>) calculated for C<sub>17</sub>H<sub>18</sub>N<sub>3</sub>O<sub>5</sub>S  $m/z$  376.0967, observed  $m/z$  376.0974.

**2**: yield: 21 mg (33%), <sup>1</sup>H NMR (400 MHz, DMSO-*d*<sub>6</sub>):  $\delta$ /ppm 9.06 (br, 1H), 8.89 (br, 1H), 8.17 (br, 1H), 8.05 (d,  $J_H = 8.4$  Hz, 2H), 7.93 (d,  $J_H = 8.4$  Hz, 2H), 7.65 (d,  $J_H = 8.8$  Hz, 2H), 7.03 (d,  $J_H = 8.8$  Hz, 2H), 4.40–3.89 (m, 3H), 3.86 (d-d,  $J_H = 6.4$  Hz, 1H), 3.35 (m, 1H), 2.85, 2.72 (m, 2H). HRMS (FAB<sup>+</sup>) calculated for C<sub>19</sub>H<sub>21</sub>N<sub>4</sub>O<sub>6</sub>S  $m/z$  433.1182, observed  $m/z$  433.1181.

**4**: yield: 30 mg (34%), <sup>1</sup>H NMR (400 MHz, DMSO-*d*<sub>6</sub>):  $\delta$ /ppm 8.62 (br, 1H), 8.08 (br, 1H), 7.96 (d,  $J_H = 8.4$  Hz, 2H), 7.87 (d,  $J_H = 8.4$  Hz, 2H), 7.57 (d,  $J_H = 8.8$  Hz, 2H), 6.98 (d,  $J_H = 8.8$  Hz, 2H), 4.43–3.86 (br, 3H), 3.32 (m, 1H), 3.28 (m, 2H), 2.84, 2.71 (m, 2H), 2.59 (m, 2H), 1.56 (m, 4H), 1.37 (m, 2H). HRMS (FAB<sup>+</sup>) calculated for C<sub>23</sub>H<sub>29</sub>N<sub>4</sub>O<sub>6</sub>S  $m/z$  489.1808, observed  $m/z$  489.1805.

Detailed experimental procedures of EDANS-ONH<sub>2</sub> and FITC-ONH<sub>2</sub> are in Supporting Information.

EDANS-ONH<sub>2</sub> (**6**): yield: 10 mg (77%), <sup>1</sup>H NMR (400 MHz, DMSO-*d*<sub>6</sub>):  $\delta$ /ppm 8.38 (m, 1H), 8.13 (d,  $J_H = 8.8$  Hz, 1H), 8.07 (d,  $J_H = 8.4$  Hz, 1H), 7.92 (d,  $J_H = 7.2$  Hz, 1H), 7.31 (dd,  $J_H = 7.2$  Hz,  $J_H = 8.4$  Hz, 1H), 7.26 (dd,  $J_H = 7.6$  Hz,  $J_H = 8.4$  Hz, 1H), 6.57 (d,  $J_H = 8.0$  Hz, 1H), 4.42 (s, 2H), 3.45 (t,  $J_H = 6.0$  Hz, 2H), 3.31 (t,  $J_H = 6.0$  Hz, 2H). HRMS (FAB<sup>+</sup>): calculated for C<sub>14</sub>H<sub>17</sub>N<sub>3</sub>O<sub>5</sub>S  $m/z$  340.089; observed  $m/z$  340.100.

FITC-ONH<sub>2</sub> (**7**): yield: 35 mg (83%), <sup>1</sup>H NMR (400 MHz, DMSO-*d*<sub>6</sub>):  $\delta$ /ppm 7.95 (s, 1H), 7.73 (br, 1H), 7.12 (d,  $J_H = 8.8$  Hz, 1H), 6.65 (d,  $J_H = 8.8$  Hz, 2H), 6.52 (s, 2H), 6.48 (d,  $J_H = 8.8$  Hz, 2H), 3.95 (s, 2H), 3.61 (s, 2H), 3.34 (br, 2H). HRMS (FAB<sup>+</sup>): calculated for C<sub>25</sub>H<sub>22</sub>N<sub>4</sub>O<sub>7</sub>S  $m/z$  523.13; observed  $m/z$  523.13.

**Post-affinity Labeling Modification of hCAII (One-Pot P-ALM).** hCAII (3.5 mg) was dissolved in 50 mM HEPES buffer (1.4 mL, pH 7.2). The concentration of hCAII was determined by absorbance at 280 nm using the molar extinction coefficient (54 000 M<sup>-1</sup> cm<sup>-1</sup>). The labeling reagent **3** (0.15 mg, 0.30  $\mu\text{mol}$ , 2.5 equiv to hCAII) in 1.6  $\mu\text{L}$  of DMSO was slowly added to the hCAII solution, and the reaction mixture was incubated at 25 °C. After 3 days, carboxymethyl-oxyamine (CM) **5** (20–100 equiv to hCAII) was slowly added to the mixture, and it was incubated again for 24 h at 45 °C. In the case of the aminoxy-fluorophores, 1.4 mg aminoxy-EDANS **6** (2.4  $\mu\text{mol}$ , 20

equiv to hCAII) or 1.3 mg of aminoxy-FITC **7** (2.4  $\mu\text{mol}$ , 20 equiv to hCAII) was used. The yield for the labeling reaction and the exchange reaction were determined by MALDI-TOF mass spectra, where the reaction percentage was calculated by dividing the target peak intensity by the total mass peak intensity due to hCAII's. Excess amount of the labeling reagent and the aminoxy-fluorophore were removed by gel filtration chromatography (TOYO PEARL: 258 cm) eluted with 50 mM HEPES buffer pH 7.2 and the labeled/modified hCAII mixture was collected.

**Preparation of the Randomly Dansyl-Modified hCAII.** To a solution of hCAII (3.0 mg) in 3.0 mL of Tris HCl buffer (25 mM, pH 8.5) was added a solution of dansyl chloride (0.81 mg, 3  $\mu\text{mol}$ , 30 equiv to hCAII) in 40  $\mu\text{L}$  of acetone. The mixture was incubated at 4 °C for 48 h in the dark and then dialyzed against 50 mM HEPES pH 7.2 to yield the randomly dansyl-modified hCAII. It was estimated that one hCAII was modified with approximately 1.5 dansyl unit on the average by absorbance at 280 and 336 nm using molar extinction coefficient ( $\epsilon_{280} = 54\,000\ \text{M}^{-1}\ \text{cm}^{-1}$  and  $\epsilon_{336} = 5700\ \text{M}^{-1}\ \text{cm}^{-1}$ ).

**Enzyme Activity Assay.**<sup>19</sup> The hydrolytic activity assay of hCAIIs was performed on UV-vis spectrum at 25 °C in 50 mM HEPES buffer (pH 7.2) using a quartz cell with 1.0 cm path length. Initial rates of *p*-nitrophenyl acetate hydrolysis were determined by the increase of the absorbance at 348 nm ( $\Delta\epsilon = 1090\ \text{M}^{-1}\ \text{cm}^{-1}$ ) for the released *p*-nitrophenolate as a product. The concentration of all hCAIIs was fixed at 1.0  $\mu\text{M}$ . The concentrations of **3**-labeled-hCAII and CM-hCAII were corrected by absorbance at 280 nm using the molar extinction coefficient, 65 700  $\text{M}^{-1}\ \text{cm}^{-1}$  and 71 000  $\text{M}^{-1}\ \text{cm}^{-1}$ , respectively. In the case of EDANS-hCAII and FITC-hCAII, the labeled/modified hCAII mixture solution was used, and the concentrations of EDANS-hCAII and FITC-hCAII were corrected by absorbance at 280 and 336 nm/490 nm using the molar extinction coefficient:  $\epsilon_{280} = 72\,000\ \text{M}^{-1}\ \text{cm}^{-1}$  and  $\epsilon_{336} = 5700\ \text{M}^{-1}\ \text{cm}^{-1}$  for EDANS-hCAII,  $\epsilon_{280} = 94\,000\ \text{M}^{-1}\ \text{cm}^{-1}$  and  $\epsilon_{494} = 68\,000\ \text{M}^{-1}\ \text{cm}^{-1}$  for FITC-hCAII, respectively. Substrate concentrations were varied from 0.2 to 20 mM, and initial rates were plotted against substrate concentrations. The stock solution of *p*-nitrophenyl acetate (100 and 500 mM) was prepared with acetonitrile. Kinetic parameters were obtained by the least-squares curve-fitting analysis with Michaelis–Menten equation (eq 1) using Kaleida Graph (Synergy Software).

$$V_0 = k_{\text{cat}} \cdot [E]_0 [S] / ([S] + K_m) \quad (1)$$

where  $V_0$  represents initial rate of hydrolysis,  $k_{\text{cat}}$  and  $K_m$  represent first-order rate constant from the catalyst–substrate complex and Michaelis–Menten constant, respectively.  $[E]_0$  and  $[S]$  represent the initial concentrations of hCAIIs and substrate, respectively.

**Fluorescence Titration Experiment.** Fluorescence titration experiments of benzenesulfonamide analogues were performed at 25 °C in 50 mM HEPES buffer (pH 7.2) using a quartz cell. The concentrations of EDANS-hCAII and FITC-hCAII were fixed at 1.0, 0.5 (only in the case of the pair of FITC-hCAII and NB), or 0.1  $\mu\text{M}$  (only in the case

of the pair of FITC-hCAII and ET). The corresponding benzenesulfonamide analogue was added dropwise to the modified hCAII solution, and emission spectra were measured ( $\lambda_{\text{ex}} = 336\ \text{nm}$  for EDANS-hCAII and  $\lambda_{\text{ex}} = 490\ \text{nm}$  for FITC-hCAII):  $[ET] = 0\text{--}1.5\ \mu\text{M}$ ;  $[NB] = 0\text{--}10\ \mu\text{M}$ ;  $[SA] = 0\text{--}20\ \mu\text{M}$ ;  $[BS] = 0\text{--}20\ \mu\text{M}$ ;  $[SA1] = 0\text{--}1.5\ \text{mM}$ ;  $[PB] = 0\text{--}40\ \text{mM}$ ;  $[SA2] = 0\text{--}40\ \text{mM}$ . An average value of three measurements was plotted for each point. Fluorescence titration curves ( $\lambda_{\text{em}} = 477\ \text{nm}$  for EDANS-hCAII and 520 nm for FITC-hCAII) were analyzed with the nonlinear curve-fitting analysis or the Benesi–Hildebrand relationship to evaluate  $K_a$  values.

Fluorescence anisotropy values ( $r$ ) of EDANS-hCAII and FITC-hCAII were evaluated from the following equation:  $r = (I_V - G \times I_H) / (I_V + 2G \times I_H)$ , where  $I_V$  and  $I_H$  are the fluorescence intensities ( $\lambda_{\text{em}} = 480\ \text{nm}$ ) observed through polarizers parallel and perpendicular to the polarization of the exciting light ( $\lambda_{\text{ex}} = 330\ \text{nm}$ ), respectively, and  $G$  is a correction factor to account for instrumental differences in detecting emitted compounds.<sup>24</sup>

**Peptide Mapping Experiment and Sequencing.**<sup>11c</sup> The EDANS-hCAII (including labeled hCAII) solution was diluted with 100 mM  $(\text{NH}_4)_2\text{CO}_3$ , pH 8.5 containing 2 M urea. Lysyl endopeptidase (LEP) was added so that the LEP/substrate ratio was 1/50 (w/w), and the digestion was allowed to proceed at 37 °C overnight. The digested peptides were separated by HPLC using YMC-Pack ODS-A column (4.6  $\phi$   $\times$  250 mm). HPLC solvents employed were acetonitrile containing 0.1% trifluoroacetic acid (TFA) (solvent A) and water containing 0.1% TFA (solvent B). HPLC analysis was carried out using a 5–55% linear gradient in solvent A over 30 min (flow rate = 1.0 mL/min). The HPLC peak was monitored by both UV absorbance at 220 nm and fluorescence at 490 nm ( $\lambda_{\text{ex}} = 340\ \text{nm}$ ), and each fraction was analyzed by MALDI-TOF MS. Among them, the fluorescent peptide peaks ( $R_t$ : 30, 42, 44 min) were conducted with tandem mass–mass analysis (Bruker, PSD (Post Source Decay) mode) to determine the sequence by PSD method using Biotoools software.

**Acknowledgment.** We gratefully thank Mr. Hiroya Hokazono for the analysis of MALDI-TOF mass spectroscopy. N.K and E.N. are JSPS fellows for Japanese Junior Scientists.

**Supporting Information Available:** Synthesis of P-ALM reagent **1**, **2**, **4**, aminoxy derivative **6**, **7**, UV–visible and fluorescence spectra of EDANS-/FITC-hCAII, the full amino acid sequence of native hCAII, MS–MS analysis data of EDANS-hCAII, fluorescence titration profile of the relative intensity change ( $I/I_0 - 1$ ) versus the inhibitor concentration for FITC-hCAII, fluorescence anisotropy data of EDANS-/FITC-hCAII. This material is available free of charge via the Internet at <http://pubs.acs.org>.

JA057926X

(24) Vinson, V. K.; Cruz, E. M.; Higgs, H. N.; Pollard, T. D. *Biochemistry* **1998**, *37*, 10871–10880.